Journal of Materials Chemistry B

Accepted Manuscript

ROYAL SOCIETY OF CHEMISTRY

www.rsc.org/materialsB

Journal Name

RSCPublishing

ARTICLE

Molybdenum Disulfide-Based Amplified Fluorescent DNA Detection Using Hybridization Chain Reactions

Cite this: DOI: 10.1039/xoxxoooooox

Jiahao Huang [a†], Lei Ye [b†], Xiang Gao [a], Hao Li [b], Jianbin Xu [b*], and Zhigang Li [a*]

Received ooth January 2012,
Accepted ooth January 2012

DOI: 10.1039/xoxxoooooox

www.rsc.org/

We report a novel MoS_2-based fluorescent biosensor for DNA detections via hybridization chain reactions (HCRs). As an emerging nanomaterial, MoS_2 has excellent fluorescence quenching ability and distinct adsorption properties toward single- and double-stranded DNA. In the sensing method, MoS_2 nanosheets are used to suppress the background signal and control the "on" and "off" of fluorescence emission of the detection system with and without the presence of the target DNA. In addition, the signal generation is amplified through the target-triggered HCRs between two hairpin probes. The employment of MoS_2 and HCRs guarantees the high sensitivity of the detection strategy with the detection limit of 15 pM. The biosensor also exhibits very good selectivity over mismatched DNA sequences. The detection takes place in solutions and requires only one "mix-and-detect" step. The high sensitivity, selectivity, and operational simplicity demonstrate that MoS_2 can be a promising nanomaterial for versatile biosensing.

Introduction

The detection of sequence-specific oligonucleotides plays essential roles in a variety of areas, including life science, disease genetics, and pharmacogenomic studies.[1-3] In the past decades, tremendous efforts and progress have been made in developing efficient methods for sensitive, selective, simple, and cost-effective DNA detections. Among all the properties, sensitivity is one of the most important and of great concern in biosensor design because the target concentration can be extremely low in real biosamples.[4] To improve the sensitivity, a popular way is to use enzymes to duplicate the DNA target or amplify the response signal. Polymerase chain reaction (PCR),[5] ligase chain reaction (LCR),[6,7] rolling circle amplification (RCA),[8-10] and nuclease-assisted target regeneration methods,[11,12] are some representative enzyme-aided, highly sensitive schemes. However, the enzymes employed in these methods are expensive, usually sequence-dependent, and sometimes require complicated protocols, which may hinder the applications of these methods. Practically, it is highly desirable to develop enzyme-free strategies for sensitive DNA detection.

With the advances of nanotechnology, many enzyme-free, yet sensitive detection approaches have been developed using nanomaterials, such as gold nanoparticle (GNPs), quantum dots (QDs), carbon nanotubes (CNTs), silicon nanowires (SiNWs), and graphene. As a promising zero-dimensional nanomaterial, GNPs have been used for sensitive detections of DNA,[13] RNA,[14] proteins,[15] and small molecules,[16] due to their high extinction coefficients and special optical properties. QDs also possess remarkable optical properties, such as broad absorption spectra, narrow emission spectra, high quantum yield, and outstanding photostability, which make them possible to replace the traditional organic dyes for fluorescence generation.[17,18] CNTs and SiNWs are one-dimensional nanomaterials. They surpass GNPs and QDs in terms of many electrical and physical properties and are good candidates for highly sensitive biodetections.[19-21] In the past a few years, graphene, a two-dimensional, single layer carbon material, has attracted a lot of attention as a fascinating building block for versatile biosensor fabrications due to its outstanding optical,[22-24] electrochemical,[25,26] and electronic[27,28] properties. Moreover, graphene has unique fluorescence quenching ability, distinct affinities to single- and double-stranded DNA, and good biocompatibility compared with other low dimensional nanomaterials.[29-31]

Very recently, another two-dimensional nanomaterial, molybdenum disulfide (MoS_2), has received increasing attention as an emerging nanomaterial.[32] MoS_2 has similar structure to graphene and shares many graphene's merits. On the other hand, it has some excellent properties associated with transition-metal dichalcogenides. Particularly, MoS_2 is a highly efficient fluorescence quencher. MoS_2-based fluorescence biosensing systems[33] have been reported to show better sensitivity than graphene-based methods.[34,35] In addition, MoS_2 bears very good properties for DNA absorption without further surface modification, which is superior to

graphene.[36-38] Therefore, MoS_2 is expected to be a promising candidate for biosensing. Unfortunately, little work has been conducted to employ MoS_2 for amplified biodetections. Extensive work is required to explore the applications of MoS_2 in biosensing.

In this work, we report a MoS_2-based, sensitive, and simple method for DNA detection using hybridization chain reactions (HCRs). In the sensing system, two complementary hairpin DNA probes, HP1 and HP2, are employed. HP1 is labeled with a fluorophore for fluorescence generation. The hairpin probes are specially designed such that the target DNA can open HP1 and initiate HCRs between HP1 and HP2. MoS_2 is wisely used to turnoff (without the target) or restore (in the presence of the target) the fluorescence based on its discriminative adsorption behaviors toward the hairpin DNA probes and HCR products. In this method, HCRs are used to amplify the fluorescence emission and MoS_2 is employed to reduce the background signal. Therefore, it is a highly sensitive strategy. The detection limit was determined to be 15 pM. Another advantage of the proposed method is that MoS_2 nanosheets in solutions act as a convenient platform for HCRs, which avoids some problems in HCRs-assisted solid-phase methods,[39-42] such as tedious immobilization procedures, slow binding dynamics, and high steric hindrance. Moreover, the sensing method is enzyme-free, selective, and operationally convenient.

Experimental section

Materials

The hairpin probes (HP1 and HP2), target DNA, and mismatched DNA sequences were synthesized by TaKaRa Bio Inc. (Dalian, China), as listed in Table S1. HP1 is labeled with a fluorophore, FAM. Both HP1 and HP2 have a stem of 18 bps and a loop of 6 nts with an extra anchoring tail of 6 nts, as shown in Fig. 1 and Table S1. The sequences of HP1 and HP2 are complementary in a staggered configuration (Table S1), such that they would hybridize when HP1 is opened by the target DNA. Bulk MoS_2 (single crystal) was purchased from SPI Supplies (PA, USA). Hydrazine hydrate, naphthalene, anhydrous tetrahydrofuran, and sodium were all purchased from Aldrich (St. Louis, MO, USA). All other reagents were of analytical grade and used without further purification or modification. All the solutions were prepared with ultrapure water obtained from a NANOpure Diamond (Barnstead Int., Dubuque, IA) source.

Preparation of MoS_2 nanosheets

MoS_2 nanosheets were fabricated using solution exfoliation approach.[43] 0.8 g bulk MoS_2 and 15 mL hydrazine hydrate were sealed in an autoclave and heated at 130 ℃ for 48 h. Then the product of expanded MoS_2 was washed three times by water and dried at 120 ℃ for 10 h. 0.35 g sodium, 0.96 g naphthalene, and 40 mL anhydrous tetrahydrofuran (fresh redistilled by sodium) were stirred for 2 h in ice-water bath in argon atmosphere until the solution became dark blue. Pre-expanded MoS_2 powder (0.8 g) was then added to the dark blue solution and the mixture was further stirred for 5 h. After the reaction, the product was washed five times by anhydrous tetrahydrofuran. Distilled water (100 mL) was then added to the intercalated sample. The mixture was sonicated in a low-power sonic bath (60 W) for 30 min to form a homogeneous suspension. The mixture was centrifuged at 10,000 r.p.m. for 15 min for several cycles to remove excess impurity, and then at 12,000 r.p.m. for 15 min in the last cycle.

Fluorescence Measurement

Fluorescence measurements were performed using a F4500 fluorometer (Hitachi, Japan). According to the fluorescent property of FAM labeled on HP1, the excitation and emission wavelengths were set at 490 and 520 nm. The slit width for both excitation and emission was set at 5 nm. To record the fluorescence emission spectra, samples were excited by a 490 nm light and scanned from 510 to 600 nm with a step of 1 nm. All the solutions were of 600 μL and prepared by mixing 50 nM HP1, 50 nM HP2, and a certain amount of MoS_2 nanosheets in the reaction buffer, which consisted of 50 mM $MgCl_2$ and 1 mM Tris-HCl with pH value equal to 8.0. All the samples were incubated at 24 ℃ for at least 10 min before the experiments.

Results and discussion

Working mechanism

The detection principle of the proposed biosensor is illustrated in Fig. 1. In the sensing method, MoS_2 nanosheets and two hairpin DNA probes, i.e., FAM-labeled HP1 and HP2, are employed. MoS_2 is reported to be able to not only absorb single-stranded DNA in a selective manner but also quench the fluorescence signal efficiently. In the absence of the target DNA, HP1 and HP2 are adsorbed on the surface of MoS_2 nanosheets due to the strong binding force between the nucleobases in their anchoring ends and MoS_2.[33a,b] Since MoS_2 nanosheets exhibit excellent fluorescence quenching ability, the fluorescence emission of FAM labeled on HP1 should be very weak and the background signal is expected to be low. When the target DNA is introduced, it hybridizes with the anchoring end and stem part of HP1. This opens the hairpin structure of HP1 and causes the rest sequences of HP1 to bind with parts of HP2. Similarly, after HP2 is opened, the exposed part of HP2 hybridizes with the complementary sequences of another HP1. Such HCRs can generate a long chain of HP1-HP2 duplex led by the target DNA. In the long chain complex, all the nucleobases are wrapped by the helical backbones and their interactions with MoS_2 become weak. This leads to the desorption of the long HP1-HP2 duplex from MoS_2 nanosheets and the recovery of the fluorescence emission of FAM. Theoretically, a small amount of target DNA can trigger the formation of many such long chains. Since each chain can generate very strong fluorescence signal, the proposed sensing method is expected to be highly sensitive.

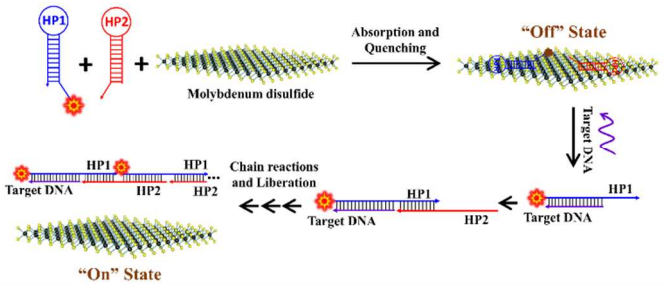

Fig.1 Detection principle of the proposed strategy. Two hairpin DNA probes, HP1 and HP2, and MoS_2 nanosheets are employed. HP1 is labeled with FAM. Without the target DNA, HP1 and HP2 are adsorbed by MoS_2 due to the strong interaction between single-stranded sequences (the anchoring ends of HP1 and HP2) and MoS_2, and the fluorescence is quenched. When the target DNA is introduced, it hybridizes with HP1 and consequently initiates the hybridization chain reactions (HCRs) between HP1 and HP2. The HCR products,

long double-stranded DNA (dsDNA), are released due to the weak dsDNA-MoS_2 interaction. This leads to the recovery of fluorescence emission. In this method, the detection sensitivity is enhanced through the reduced background signal (MoS_2) and amplified fluorescence emission (HCRs).

Characterization of MoS_2 nanosheets

MoS_2 has a layered structure of hexagons that consist of a plane of molybdenum atoms sandwiched covalently between two planes of sulfur atoms. The two typical Raman peaks, E^1_{2g} and A_{1g}, are strongly associated with the thickness of MoS_2 nanosheets. The E^1_{2g} peak is attributed to the in-plane relative motion between the two sulfur atoms and the molybdenum atom, while the A_{1g} peak is attributed to the out-of-plane vibration of the two sulfur atoms in opposite directions.[44] E^1_{2g} and A_{1g} peaks in frequency approach each other as the number of layers decreases.[45] The Raman spectrum was employed to identify the MoS_2 nanosheets using a 532-nm excitation line. As shown in Fig. 2a, the E^1_{2g} peak of the MoS_2 nanosheets shifted to 384.3 cm^{-1}, while the A_{1g} peak shifted to 403.3 cm^{-1} compared to bulk MoS_2 (for bulk MoS_2, E^1_{2g} and A_{1g} peaks are at ~383 and ~408 cm^{-1}, respectively[46]). This is consistent with that of mechanically exfoliated single-layer MoS_2 nanosheets.[47] These shifts are mainly attributed to the structure changes or long-range columbic interlayer interactions for E^1_{2g} [45] and the decrease of the force constant resulted from the weakening of the interlayer van der Waals force between layers for A_{1g}.[46] The morphology of the exfoliated MoS_2 nanosheets was further analyzed by atomic force microscopy (AFM). The thickness of these nanosheets was tested by using the tapping mode AFM image of the MoS_2 nanosheets deposited on a SiO_2/Si substrate, as shown in Fig. 2b. The topographic height was around 1 nm, which agrees with the typical height of single-layer MoS_2 nanosheets (between 0.6 and 1.0 nm).[48] The average size of the MoS_2 nanosheets was about 3 μm.

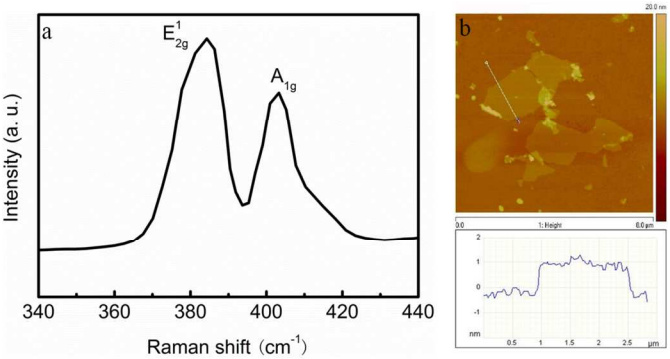

Fig.2 Characterization of MoS_2 nanosheets. (a) and (b) are the Raman spectra and AFM image of the solution-exfoliated MoS_2 nanosheets deposited on SiO_2/Si substrates, respectively.

Transmission electron microscope (TEM) was then applied to examine the exfoliated MoS_2 nanosheets suspended on a lacey carbon TEM grid. The low magnification TEM image in Fig. 3a shows the existence of wrinkled MoS_2 nanosheets. The overlap and slight corrugations were due to the large aspect ratio of two dimensional single-layer materials.[49] Fig. 3b displays a high-resolution TEM (HRTEM) image taken from part of the exfoliated MoS_2 nanosheets. The inset shows the selected area electron diffraction (SAED) patterns of the exfoliated MoS_2 nanosheets, which indicate that the MoS_2 nanosheets possessed high crystallinity, as judged from the characteristic honeycomb lattice.

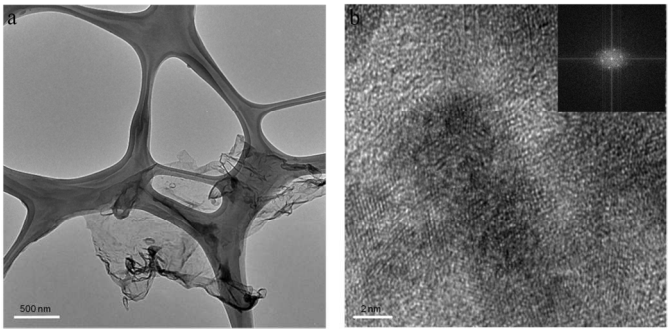

Fig.3 TEM images of MoS_2 nanosheets. (a) Low magnification TEM image of the MoS_2 nanosheets. (b) A typical HRTEM image taken from part of the MoS_2 nanosheets. The inset shows the SAED pattern from the MoS_2 surface.

Fluorescence quenching ability of MoS_2 nanosheets

The quenching capability of MoS_2 nanosheets is critical for the proposed detection method. To verify the performance of MoS_2 nanosheets, the fluorescence responses of samples containing HP1 and HP2 at different MoS_2 concentrations were studied. Fig. 4a shows the time response of the fluorescence intensity at the peak emission wavelength (λ=520 nm) when the sample containing 50 nM HP1 and 50 nM HP2 was examined with successive additions of MoS_2 nanosheets (concentration varied from 0 to 65 μg/mL). It is seen that the quenching processes completed within a very short time (about one second), which is much faster than those caused by GNPs, CNTs, and GO.[19,22,30] This might result from the large planar surface area and superb adsorption property of MoS_2.[30,50] Fig. 4b displays the corresponding fluorescence spectra right after the addition of MoS_2 nanosheets at each step. It is found that the fluorescence signal decreased with increasing MoS_2 concentration. Fig.4c depicts the quenching efficiency of MoS_2 as a function of MoS_2 concentration. The quenching efficiency is defined as $(F_0\text{-}F)/F_0$, where F and F_0 are the fluorescence intensities of the solutions at the wavelength of λ=520 nm with and without MoS_2, respectively. The quenching efficiency reached about 95% when the MoS_2 concentration was higher than 60 μg/mL, which was chosen for the other experiments in this work. The fluorescence quenching of FAM is mainly due to the long range resonance energy transfer from the donor (FAM) to the accepter (MoS_2).[51,52] Table S2 lists the quenching performance of different nanomaterials in some DNA-based biosensing systems.

Detection feasibility

The feasibility of the proposed method was tested by introducing the target DNA into the sensing system. Fig. 5 shows the fluorescence intensity (Fig. 5a) and fluorescence emission spectra (Fig. 5b) for different samples. As depicted in Fig. 5a, the fluorescence intensity of the sample containing 50 nM HP1, 50 nM HP2, and 60 μg/mL MoS_2 nanosheets was about 262 a.u. and remained nearly unchanged in the whole reaction process. Similar fluorescence response was observed for the sample containing 50 nM HP1 and 60 μg/mL MoS_2

because HP1 was the sole source of fluorescence. However, when the two samples were tested with 35 nM target DNA, the

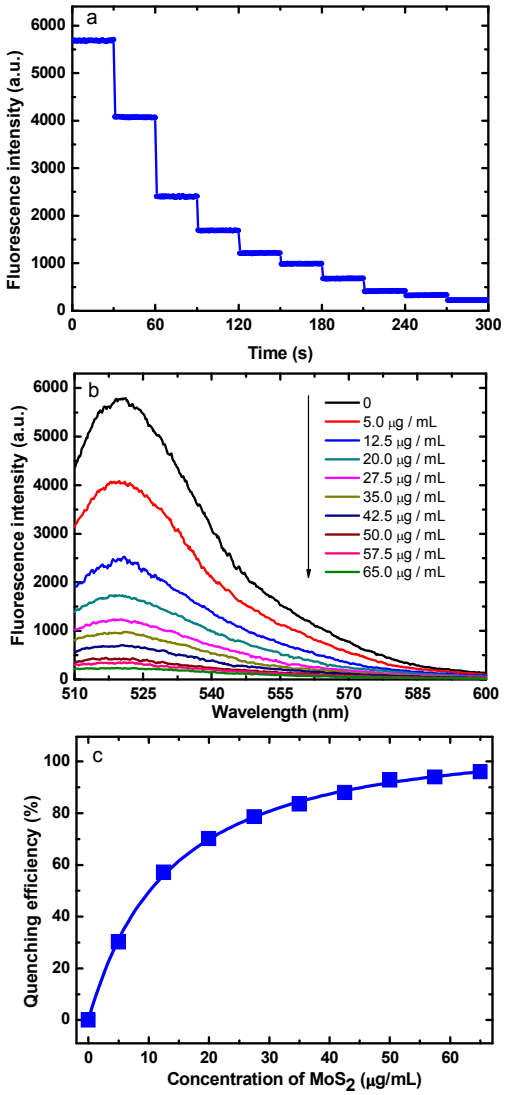

Fig.4 Effects of MoS_2 concentration on the fluorescence response of the sensing system. (a) Time response of the fluorescence intensity at 520 nm emission wavelength. (b) Fluorescence emission spectra. (c) Quenching efficiency, $(F_0\text{-}F)/F_0$, as a function of MoS_2 concentration (F and F_0 are the fluorescence intensities of the DNA solutions at 520 nm emission wavelength with and without MoS_2, respectively).

fluorescence responses behaved quite differently. For the sample containing MoS_2 and HP1 only, the signal increased slightly and approached 760 a.u. after about 2 h. For the proposed sensing system, the response signal increased quickly with time. The fluorescence intensity reached 2968 a.u. 3 h after the same amount of target DNA was added into the solution. The increasing fluorescence signal was the consequence of the formation of the HCRs products (HP1-HP2 duplex) and their subsequent detachment from MoS_2 nanosheets, which confirms the reaction mechanism in Fig. 1. Compared with the case containing HP1 only, the proposed sensing system led to 5.3-fold increase in the net signal gain after 3 h reaction (Fig. 5a), which is calculated as $(F_{HP1+HP2+MoS2+Target}\text{-}F_{HP1+HP2+MoS2})/(F_{HP1+MoS2+Target}\text{-}F_{HP1+MoS2})$ with F being the fluorescence intensity at the wavelength of λ=520 nm. Therefore, the current detection scheme has the potential to strengthen the detection sensitivity. It is noted that the HCRs take a couple of hours, which is much longer than the fluorescence quenching time of MoS_2 (Fig. 4). This is a drawback of the current method.

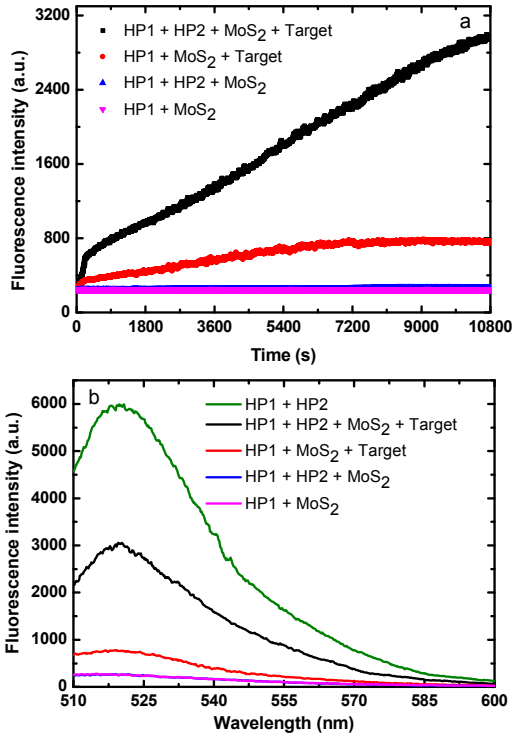

Fig.5 Fluorescence responses of samples with and without the addition of HP2 and/or the target DNA. (a) Kinetic studies. (b) Fluorescence emission spectra. The concentrations of hairpin DNA probes and MoS_2 in all the samples were 50 nM and 60 μg/mL, respectively. They all reacted at 24 ^{o}C for 3 h with or without the addition of 35 nM target DNA.

Detection sensitivity

The sensitivity of the detection strategy was investigated by varying the target concentration. Fig. 6a shows the fluorescence spectra of the sensing system upon the addition of target DNA after incubation for 3 h. It is seen that the fluorescence intensity increased with increasing target concentration. Fig. 6b plots the fluorescence intensity at the wavelength of 520 nm for target concentration ranging from 30 pM to 5 nM. The response signal appeared to be linearly proportional to the target concentration in the range from 0 to 200 pM, as shown in the inset. Based on the linear fit, the limit of detection (LOD) was theoretically determined as 15 pM, which is the value of $3\sigma/S$ (σ is the standard deviation of the background signal and S is the slope of the linear regression line shown in the inset of Fig. 6b). This LOD is one or two orders of magnitude lower than GNPs-, CNT- and GO-based approaches.[13,19,35]

As HCRs also contributed to the sensitivity through amplifying the response signal, experiments involving only HP1 and MoS_2 were conducted for comparison, where HCRs were not involved. Fig. 7 demonstrates the fluorescence spectra at different target concentrations (Fig. 7a) for the

sample without HP2 and the fluorescence intensities at the wavelength of 520 nm (Fig. 7b) 3 h after the target was introduced. The LOD of this approach without HCRs was theoretically obtained as 1.8 nM, which is 120 times poorer than that of the present strategy. Therefore, the reduced background signal achieved by MoS_2 and amplified fluorescence generation due to HCRs guaranteed the high sensitivity of the current sensing method.

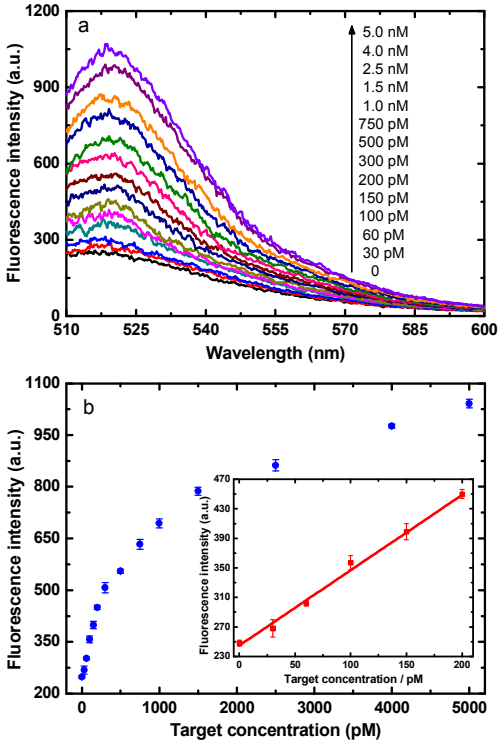

Fig.6 Fluorescence response of the proposed sensing system (50 nM HP1, 50 nM HP2, and 60 μg/mL MoS_2) in the presence of different amounts of target DNA. (a) Fluorescence emission spectra. (b) Fluorescence intensity at the emission wavelength of 520 nm as a function of target DNA concentration. The inset shows the linear relationship in the concentration range from 0 to 200 pM. All the samples reacted at 24 ^{o}C for 3 h before measurement.

Detection selectivity

The selectivity of the proposed system was also examined by scrutinizing the sensing system with non-specific DNA sequences, including single base-, three base-mismatched, and random DNA sequences (Table S1). The fluorescence intensities after the addition of 10 nM different DNA sequences are depicted in Fig. 8a. It is seen that the target DNA produced a significantly high fluorescence signal compared with those caused by the mismatched DNA sequences. Fig. 8b shows the fluorescence intensities at the emission wavelength of 520 nm, where the signals were scaled by the background signal. The fluorescence intensities for the target, single-base-mismatched, three-base-mismatched, and random DNA were about 5.15, 1.87, 1.63, and 1.24 times the background signal, respectively. The excellent selectivity is attributed to the stable structure of HP1 and unfavorable hybridizations between mismatched DNA sequences and HP1.

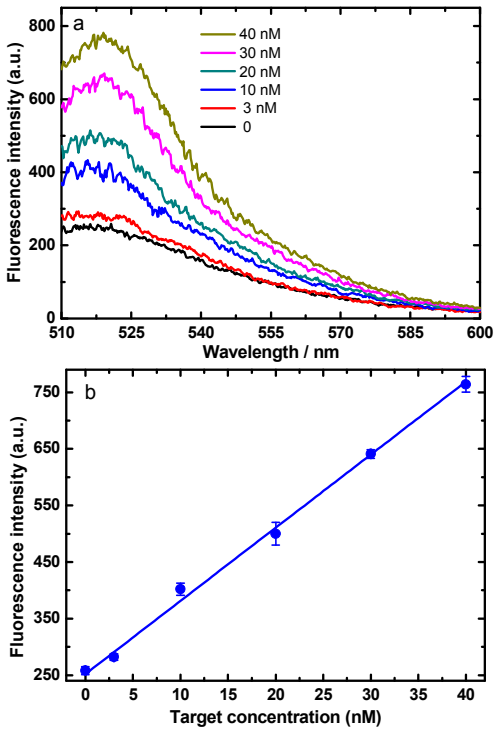

Fig.7 Fluorescence response of samples without HP2 and HCRs (50 nM HP1 and 60 μg/mL MoS_2) for different concentrations of the target DNA. (a) Fluorescence emission spectra. (b) Relationship between the fluorescence intensity at the emission wavelength of 520 nm and the target DNA concentration ranging from 0 to 40 nM. All the samples reacted at 24 ^{o}C for 3 h before measurement.

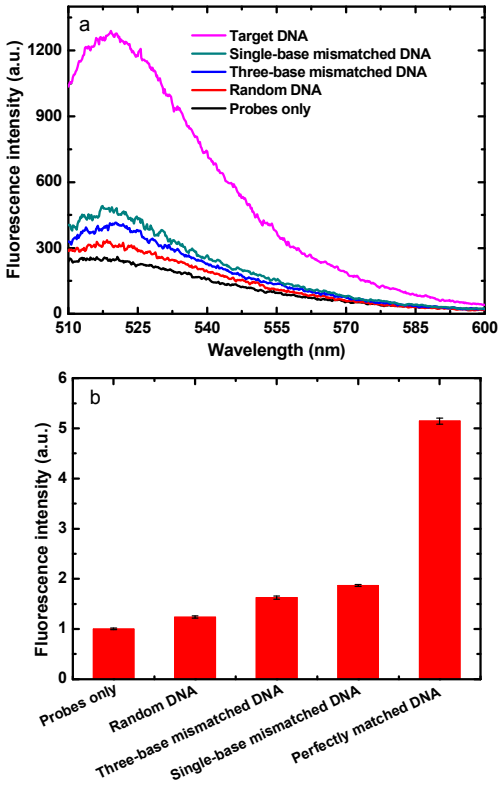

Fig.8 Specificity of the sensing approach against mismatched DNA sequences. (a) Fluorescence emission spectra. (b)

Relative fluorescence response (scaled by the background signal). All the samples reacted at 24 ^{o}C for 3 h after the addition of 10 nM different DNA sequences.

Conclusions

A one-step MoS_2-based homogeneous sensing method for sensitive DNA detections using HCRs has been proposed. In the sensing system, the target DNA triggered HCRs between two hairpin probes and generated long duplex chains, which amplified the response signal. MoS_2 was used as an excellent fluorescence quencher to greatly suppress the background signal and help improve the detection sensitivity. The detection limit of the proposed biosensor was determined as 15 pM, which was two orders of magnitude lower than the conventional scheme. This method could also discriminate the target DNA from random DNA sequence and even single-base mismatched DNA sequence with excellent specificity. The desirable sensitivity, selectivity, and simplicity of the sensing system demonstrated that MoS_2 could be a promising nanomaterial for various biosensors.

Acknowledgements

This work was supported by the Research Grants Council of the Hong Kong Special Administrative Region under Grant Nos. 615312, AoE/P-03/08, CUHK4179/10E, and N_CUHK405/12.

Notes and references

[a] Department of Mechanical and Aerospace Engineering, The Hong Kong University of Science and Technology, Clear Water Bay, Kowloon, Hong Kong, China.

[b] Department of Electronic Engineering, Materials Science and Technology Research Center, The Chinese University of Hong Kong, Shatin, New Territories, Hong Kong, China.

† J. H. Huang and L. Ye contributed equally to this work.

* E-mails: mezli@ust.hk; jbxu@ee.cuhk.edu.hk

Electronic Supplementary Information (ESI) available: [Table S1: hairpin DNA probes and other oligonucleotides used in the experiments; and Table S2: comparison of fluorescence quenching performance of different nanomaterials in some nanomaterial/DNA-based sensing systems.]. See DOI: 10.1039/b000000x/

1. J. J. McCarthy and R. Hilfiker, *Nat Biotechnol.*, 2000, **18**, 505.
2. J. H. Huang, X. F. Su and Z. G. Li, *Anal. Chem.*, 2012, **84**, 5939.
3. J. H. Huang, X. F. Su and Z. G. Li, *Sens Actuators B Chem.*, 2014, **200**, 117.
4. Y. V. Gerasimova and D. M. Kolpashchikov, *Chem. Soc. Rev.*, 2014, **43**, 6405.
5. Z. Cheglakov, Y. Weizmann, M. K. Beissenhirtz and I. Willner, *Chem. Commun.*, 2006, **30**, 3205.
6. Y. Q. Cheng, Q. Du, L. Y. Wang, H. L. Jia and Z. P. Li, *Anal. Chem.*, 2012, **84**, 3739.
7. W. Shen, H. M. Deng and Z. Q. Gao, *J. Am. Chem. Soc.*, 2012, **134**, 14678.
8. W. Zhao, M. M. Ali, M. A. Brook and Y. F. Li, *Angew. Chem. Int. Ed.*, 2008, **47**, 6330.
9. W. Xu, X. J. Xie, D. W. Li, Z. Q. Yang, T. H. Li and X. G. Liu, *Small*, 2012, **8**, 1846.
10. A. R. Gao, N. L. Zou, P. F. Dai, N. Lu, T. Li, Y. L. Wang, J. L. Zhao and H. J. Mao, *Nano Lett.*, 2013, **13**, 4123.
11. Y. Weizmann, M. K. Beissenhirtz, Z. Cheglakov, R. Nowarski, M. Kotler and I. Willner, *Angew. Chem. Int. Ed.*, 2006, **45**, 7384.
12. X. L. Zuo, F. Xia, Y. Xiao and K. W. Plaxco, *J. Am. Chem. Soc.*, 2010, **132**, 1816.
13. P. C. Ray, *Angew. Chem. Int. Ed.*, 2006, **45**, 1151.
14. F. Degliangeli, P. Kshirsagar, V. Brunetti, P. P. Pompa and R. Fiammengo, *J. Am. Chem. Soc.*, 2014, **136**, 2264.
15. H. S. Cho, E. C. Yeh, R. Sinha, T. A. Laurence, J. P. Bearinger and L. P. Lee, *ACS Nano*, 2012, **6**, 7607.
16. K. L. Ai, Y. L. Liu and L. H. Lu, *J. Am. Chem. Soc.*, 2009, **131**, 9496.
17. R. Freeman and I. Willner, *Chem. Soc. Rev.*, 2012, **41**, 4067.
18. A. M. Smith and S. M. Nie, *Nat. Biotechnol.*, 2009, **27**, 732.
19. R. H. Yang, J. Y. Jin, Y. Chen, N. Shao, H. Z. Kang, Z. Xiao, Z. W. Tang, Y. R. Wu, Z. Zhu and W. H. Tan, *J. Am. Chem. Soc.*, 2008, **130**, 8351.
20. S. Su, X. P. Wei, Y. L. Zhong, Y. Y. Guo, Y. Y. Su, Q. Huang, S. T. Lee, C. H. Fan and Y. He, *ACS Nano*, 2012, **6**, 2582.
21. E. L. Gui, L. J. Li, K. Zhang, Y. Xu, X. Dong, X. Ho, P. S. Lee, J. Kasim, Z. X. Shen, J. A. Rogers and S. G. Mhaisalkar, *J. Am. Chem. Soc.*, 2007, **129**, 14427.
22. J. H. Huang, Q. B. Zheng, J. K. Kim and Z. G. Li, *Biosens. Bioelectron.*, 2013, **43**, 379.
23. H. Jang, Y. K. Kim, H. M. Kwon, W. S. Yeo, D. E. Kim and D. H. Min, *Angew. Chem. Int. Ed.*, 2010, **49**, 5703.
24. J. H. Huang, X. Gao, J. J. Jia, J. K. Kim and Z. G. Li, *Anal. Chem.*, 2014, **86**, 3209.
25. A. Bonanni and M. Pumera, *ACS Nano*, 2011, **5**, 2356.
26. A. Bonanni, C. K. Chua, G. J. Zhao, Z. Sofer and M. Pumera, *ACS Nano*, 2012, **6**, 8546.
27. C. T. Lin, P. T. K. Loan, T. Y. Chen, K. K. Liu, C. H. Chen, K. H. Wei and L. J. Li, *Adv. Funct. Mater.*, 2013, **23**, 2301.
28. X. C. Dong, Y. M. Shi, W. Huang, P. Chen and L. J. Li, *Adv. Mater.*, 2010, **22**, 1649.
29. C. H. Lu, H. H. Yang, C. L. Zhu, X. Chen and G. N. Chen, *Angew. Chem. Int. Ed.*, 2009, **48**, 4785.
30. F. Li, H. Pei, L. H. Wang, J. X. Lu, J. M. Gao, B. W. Jiang, X. C. Zhao and C. H. Fan, *Adv. Funct. Mater.,* 2013, **23**, 4140.
31. Y. Q. Yang, A. M. Asiri, Z. W. Tang, D. Du and Y. H. Lin, *Mater. Today.*, 2013, **16**, 365.
32. (a) X. Huang, C. L. Tan, Z. Y. Yin and H. Zhang, *Adv. Mater.*, 2014, **26**, 2185. (b) H. Li, J. Wu, Z. Y. Yin and H. Zhang, *Acc. Chem. Res.* 2014, **47**, 1067. (c) X. Huang, Z. Y. Yin and H. Zhang, *Chem. Soc. Rev.,* 2013, **42**, 1934.
33. (a) C. F. Zhu, Z. Y. Zeng, H. Li, F. Li, C. H. Fan and H. Zhang, *J. Am. Chem. Soc.*, 2013, **135**, 5998. (b) J. Ge, E. C. Ou, R. Q. Yu and X. Chu, *J. Mater. Chem. B*, 2014, **2**, 625. (c) Y. Zhang, B. Zheng, C. F. Zhu, C. L. Tan, H. Li, B. Chen, J. Yang, J. Z. Chen, Y. Huang, L. H. Wang and H. Zhang, Adv. Mater. 2014, DOI: 10.1002/adma.201404568.
34. F. Li, Y. Huang, Q. Yang, Z. T. Zhong, D. Li, L. H. Wang, S. P. Song and C. H. Fan, *Nanoscale*, 2010, **2**, 1021.
35. C. H. Lu, J. Li, J. J. Liu, H. H. Yang, X. Chen and G. N. Chen, *Chem.-Eur. J*, 2010, **16**, 4889.
36. K. Liu, J. D. Feng, A. Kis and A. Radenovic, *ACS Nano*, 2014, **8**, 2504.

37. G. F. Schneider, S. W. Kowalczyk, V. E. Calado, G. Pandraud, H. W. Zandbergen, L. M. K. Vandersypen, M. K. Lieven and C. Dekker, *Nano Lett.*, 2010, **10**, 3163.
38. C. A. Merchant, K. Healy, M. Wanunu, V. Ray, N. Peterman, J. Bartel, M. D. Fischbein, K. Venta, Z. T. Luo, A. T. C. Johnson and M. Drndic, *Nano Lett.*, 2010, **10**, 2915.
39. Y. Chen, J. Xu, J. Su, Y. Xiang, R. Yuan and Y. Q. Chai, *Anal. Chem.*, 2012, **84**, 7750.
40. Z. L. Ge, M. H. Lin, P. Wang, H. Pei, J. Yan, J. Y. Shi, Q. Huang, D. N. He, C. H. Fan and X. L. Zuo, *Anal. Chem.*, 2014, **86**, 2124.
41. J. J. Zhao, C. F. Chen, L. L. Zhang, J. H. Jiang and R. Q. Yu, *Biosens Bioelectron.*, 2012, **36**, 129.
42. C. Wang, H. Zhou, W. P. Zhu, H. B. Li, J. H. Jiang, G. L. Shen and R. Q. Yu, *Biosens Bioelectron.*, 2013, **47**, 324.
43. J. Zheng, H. Zhang, S. H. Dong, Y. P. Liu, C. T. Nai, H. S. Shin, H. Y. Jeong, B. Liu and K. P. Loh, *Nat Commun.*, 2014, **5**, 2995.
44. L. Q. Su, Y. Zhang, Y. F. Yu and L. Y. Cao, *Nanoscale*, 2014, **6**, 4920.
45. C. Lee, H. Yan, L. E. Brus, T. F. Heinz, J. Hone and S. Ryu, *ACS Nano*, 2010, **4**, 2695.
46. H. Li, Q. Zhang, C. C. R. Yap, B. K. Tay, T. H. T. Edwin, A. Olivier and D. Baillargeat, *Adv. Funct. Mater.*, 2012, **22**, 1385.
47. H. Li, G. Lu, Z. Y. Yin, Q. Y. He, H. Li, Q. Zhang and H. Zhang, *Small*, 2012, **8**, 682.
48. Z. Y. Zeng, Z. Y. Yin, X. Huang, H. Li, Q. Y. He, G. Lu, F. Boey and H. Zhang, *Angew. Chem. Int. Ed.*, 2011, **50**, 11093.
49. L. H. Liu, M. M. Lerner and M. D. Yan, *Nano Lett.*, 2010, **10**, 3754.
50. M. C. Daniel, I. B. Tsvetkova, Z. T. Quinkert, A. Murali, M. De, V. M. Rotello, C. C. Kao and B. Dragnea, *ACS Nano*, 2010, **4**, 3853.
51. A. T. L. Tan, J. Kim, J. K. Huang, L. J. Li and J. X. Huang, *Small*, 2013, **9**, 3253.
52. H. D. Ha, D. J. Han, J. S. Choi, M. Park and T. S. Seo, *Small*, 2014, **10**, 3858.

For the table of contents (TOC) only

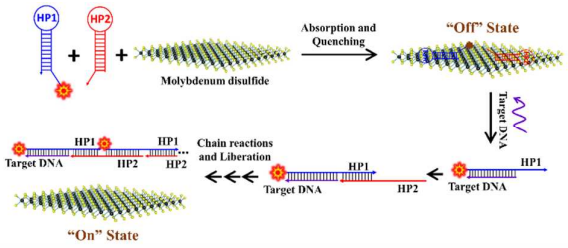

A simple, sensitive, and selective amplified fluorescence DNA detection strategy via enzyme-free molybdenum disulfide-assisted hybridization chain reactions